Regional Environmental Change (2019) 19:1777–1786
https://doi.org/10.1007/s10113-019-01496-6

ORIGINAL ARTICLE

1.5°, 2°, and 3° global warming: visualizing European regions affected by multiple changes

Susanne Pfeifer[1] · Diana Rechid[1] · Maximilian Reuter[2] · Elisabeth Viktor[1] · Daniela Jacob[1]

Received: 27 October 2017 / Accepted: 26 March 2019 / Published online: 31 May 2019

Abstract

Assessing multiple climatic and non-climatic variables affecting one region at the same time is a crucial aspect to support climate adaptation action. This publication presents a method to display relevant measures of any three adaptation relevant parameters (or optionally their projected future changes) at once on a map by allocating them to multiple transparency levels of the three primary colors of additive color mixing (red, green, and blue). The overlay of information allows the combined assessment of the regional exposures. The method is demonstrated by two examples based on an ensemble of regional climate projections analyzed for 1.5 °C, 2 °C, and 3 °C global warming periods. The first example shows the increasing number of people at risk for summer climate extremes under 1.5 °C, 2 °C, and 3 °C global warming by combining projected increases in tropical nights and summer intense precipitation days with today's population density. Under 3 °C global warming, many heavily populated areas across Europe are affected by both heat stress and summer precipitation extremes, whereas under 1.5 °C global warming, heat stress regions are restricted to southern Europe and the large settlements along the Eastern Mediterranean coast. A second example combines daily mean and minimum and maximum summer temperatures and highlights the regional expansion and the increasing robustness of projected mean summer warming with rising global warming levels, as well as the regional day to night differences of the warming signal.

Keywords EURO-CORDEX · Global warming targets · Regional climate change · Europe · Visualization method · Combined climate change indices · Combined climate impact assessment · Climate adaptation

Editor: Marc J. Metzger

Electronic supplementary material The online version of this article (https://doi.org/10.1007/s10113-019-01496-6) contains supplementary material, which is available to authorized users.

✉ Susanne Pfeifer
susanne.pfeifer@hzg.de

Diana Rechid
diana.rechid@hzg.de

Maximilian Reuter
mreuter@iup.physik.uni-bremen.de

Elisabeth Viktor
elisabeth.viktor@hzg.de

Daniela Jacob
daniela.jacob@hzg.de

[1] Climate Service Center Germany (GERICS), Helmholtz-Zentrum Geesthacht, Fischertwiete 1, 20095 Hamburg, Germany

[2] Institute of Environmental Physics, University of Bremen, Bremen, Germany

Introduction

Climate change is manifested by many interconnected aspects. In many cases, one parameter or one process is studied in isolation to reduce the complexity of the system and gain an in-depth understanding for this particular aspect. Yet, in real life, we cannot filter certain aspects; we experience climate change in its entirety and with all its components. Hence, it is just as important to consider the combination of several impacts for a region as it is to zoom in on one particular feature. The level of stress forced onto humans and their environment can increase considerably with the coincidence of several climatic changes (Zscheischler and Seneviratne 2017; Leonard et al. 2014). Even impacts that are not directly causally linked beyond the generally higher level of greenhouse gases in the atmosphere can lead to unexpected consequences or turning points when occurring in combination. Furthermore, climate change impacts might be regionally more or less problematic depending on the socio-economic and environmental setting of the concerned regions (Ritzema

and Van Loon-Steensma 2017; Olesen et al. 2011; Poumadère et al. 2005). To be able to analyze these phenomena in more detail, this publication is presenting a method to study any three parameters at once and evaluate their expected changes in combination. In addition to the possibility to examine the change of three different parameters, this method also allows for an evaluation of the robustness of the change, i.e., the level of agreement across a number of climate model projections.

The examples used here to showcase the application of the newly developed method present the evolution of the combination of three different parameters for three different scenarios: a global warming of 1.5 °C, of 2 °C, and of 3 °C. These scenarios were chosen due to their political relevance (Schleussner et al. 2016). To significantly reduce the risks and impacts of climate change, a general consensus of limiting the global temperature rise to below 2 °C compared to preindustrial levels was reached with the Paris Agreement in 2015 during COP 21. The agreement further states that efforts are pursued to reach the even more ambitious target of 1.5 °C. While it is a top priority to develop ways to drastically reduce greenhouse gases in order to slow down and ultimately stop a warming on a global scale, the unavoidable consequences of a moderate increase of global temperatures within these boundaries have to be studied and understood. This way, the implications can be assessed in advance and decision-makers can set preparations in motion according to the expected impacts. The scenario of a global temperature rise of 3 °C is included to demonstrate the worst case, failing to fulfill the Paris agreement. It is a stark reminder of the high stakes involved.

Data and methods

Climate projections

All climatic analyses presented in the following are based on climate change projections provided by the EURO-CORDEX Initiative (Jacob et al. 2014, Kotlarski et al., 2014). The data used for this study encompasses 38 simulations in total, based on the representative concentration pathways (RCP, (van Vuuren et al. 2011)). We use 11 simulations based on RCP2.6, 13 on RCP4.5 and 14 on RCP8.5.

Socio-economic data

The population density data (Gridded Population of the World, Version 4 (GPWv4)) has been taken from the Center for International Earth Science Information Network (CIESIN 2016; Doxsey-Whitfield et al. 2015). It is provided on a 30 arc-second grid raster in GeoTiff format and was regridded to the 0.11° grid of the EURO-CORDEX climate projections.

Definition of the 1.5 °C, 2 °C, and 3 °C global warming periods

To assess regional climate changes connected to a global mean temperature increase of 1.5 °C, 2 °C, and 3 °C with respect to preindustrial times, 30-year running mean averages of global mean temperatures have been calculated from all GCM simulations. The first year of exceedance of the respective temperature threshold (compared to the period of 1971–2000, plus a preindustrial temperature offset of 0.46 °C) was used as central year to define the 30-year periods representing 1.5 °C, 2 °C, and 3 °C global warming according to the method by Vautard et al. (2014). A similar method to extract 1.5 °C and 2.0 °C global warming periods from EURO-CORDEX simulations was used by Kjellström et al. (2018), but with a slightly different calculation of the preindustrial temperature offset.

With this method, a separation of the different simulations by RCP is not needed. Applied to the EURO-CORDEX simulations (date of download: 05/2017), the ensemble of simulations available to assess the 1.5 °C warming period has 38 members; for 2.0 °C, 31 members are available; and the 3.0 °C period consists of an ensemble of 16 members. To assess how the pathway to the global warming period (i.e., the time that has passed until the individual simulation has reached the global warming target) influences the projected temperature changes for Europe, Fig. 1 shows the 30-year mean projected temperature increase (a) and the 30-year annual standard deviation of projected temperature changes (b) for each simulation of the ensemble sorted by the central year when the driving GCM reaches the respective threshold of global mean temperature increase (1.5 °C, 2 °C, and 3 °C). Circles indicate RCP2.6 simulations, squares indicate RCP4.5 simulations, and triangles RCP8.5 simulations. For 1.5 °C global warming (red symbols), no distinction of both the years when the GCM reaches the 1.5 °C warming and the RCM projected temperature change and the belonging standard deviation at this period can be seen. The RCP forcing becomes more distinguishable from each other when looking at the 2.0 °C and 3.0 °C warming periods (blue and green symbols). Here, the RCP8.5 driven simulations (triangles) tend to reach the target temperature level earlier and with slightly higher standard deviations as the RCP4.5 driven simulations (squares). However, the RCM temperature change signals of the RCP2.6, RCP4.5 and RCP8.5 driven simulations for a given warming period are very similar and the differences in standard deviation and time of reaching the target are not substantial. Thus, we conclude that our approach of defining the global warming periods without separation of the RCP scenarios is valid for this application. For better comparability of the projected changes, the 1.5 °C and 2 °C ensembles have been reduced to those simulations also available for the 3 °C period. As none of the GCM simulations of RCP2.6 reaches

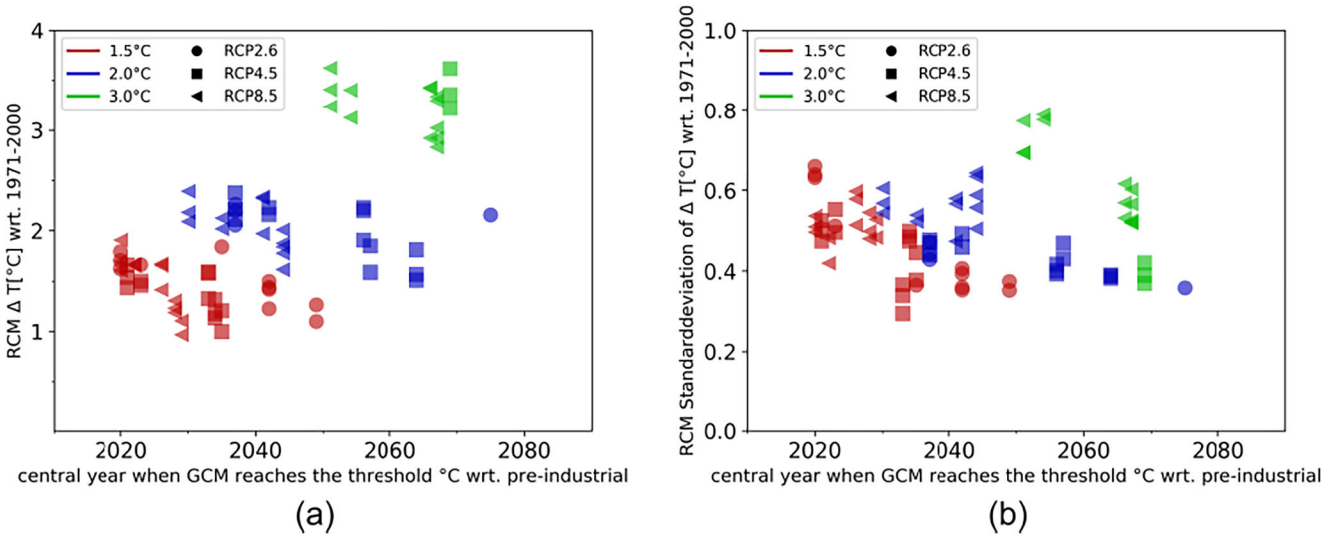

Fig. 1 **a** Projected temperature changes [°C] and **b** changes of the mean standard deviation of the annual temperatures [°C] with respect to the reference period of 1971 to 2000 for the RCM simulations (y-axes) versus the central year at which the driving GCM reaches the temperature threshold of + 1.5 °C (red), + 2.0 °C (blue) and + 3.0 °C (green) global mean warming with respect to preindustrial climate. Circles/squares/triangles represent RCP2.6/RCP4.5/RCP8.5 driven climate projections

the + 3 °C global average temperature change with respect to preindustrial climate, the resulting ensemble consists of RCP4.5 (3) and RCP8.5 (13) simulations only. The disadvantage of this ensemble reduction is that quite some information available from those simulations not reaching the 3° global warming level is lost for the analysis of 1.5° and 2° global warming consequences for Europe.

Visualization

A new method has been developed that allows the visualization of any three parameters relevant for climate impact assessment or/and their projected changes together on a map. For instance, these parameters can be a combination of projected future changes of climatic parameters and climatic parameters of today's climate and of societal/economic values such as population density or critical/vulnerable infrastructure. Each of the three parameters is represented by one of the three primary colors of additive color mixing: red (R), green (G), and blue (B). For each parameter, a "relevance" condition has to be defined. For example, the magnitude of projected climate changes to be displayed can be defined by the exceedance of a certain threshold value (e.g., increase of heat days by more than 10 days/year, decrease of summer precipitation by more than 20%) or by any other pre-defined criterion, e.g., the statistical significance of the projected changes. The relevance criterion for parameters such as population density or vulnerable infrastructure could as well be a certain threshold or fraction of area coverage to be exceeded.

In addition, the simulation agreement level (SAL) for the projected climatic parameters is introduced into the figures to account for the robustness and bandwidth of the projection ensemble and to highlight regions of very high confidence in the projected changes (high SAL) together with regions of medium or small confidence (lower SALs). It is defined as the fraction of the underlying future climate simulations, which are requested to project changes exceeding the predefined criterion. A minimum SAL that has to be exceeded (e.g., 50% of the ensemble simulations) is defined as lowest possible SAL. The SALs are separated via the transparency of the respective primary color, ordered from full transparency for the lowest SAL to full opacity for the highest SAL. Overlaying these three primary color maps results in an image which is covering the RGB color space and where regions with two or three of the parameter changes fulfilling the predefined relevance criterion with a SAL > 0 are expressed by the respective additive combination of colors.

For this purpose, we firstly normalize the three quantities to be displayed $x'(x \in [\mathrm{r}, \mathrm{g}, \mathrm{b}])$ by

$$\mathrm{x} = \frac{x' - \min(x')}{\max(x') - \min(x')}$$

An opaque RGB (red, green, blue) foreground image F can be semi-transparently overlaid over an opaque RGB background image B by alpha blending and the opaque result becomes

$$\mathrm{I} = \alpha \mathrm{F} + (1 - \alpha) B$$

Here, α corresponds to the opaqueness of F, i.e., $\alpha = 0$ represents full transparency and $\alpha = 1$ full opaqueness. Overlaying only one individual color channel, e.g., red, could be achieved by alpha blending the RGBα (red, green, blue, alpha) with the semitransparent single channel image [1, 0, 0,

r] ([0, 1, 0, g] for green or [0, 0, 1, b] for blue). However, alpha blending is not commutative, i.e., the order makes a difference. Therefore, we are interested in first combining the single channel representations of the three quantities in a commutative way resulting in one semitransparent image [R, G, B, α] to be combined via alpha blending with the background. In analogy to the combination of two semitransparent images according to Porter and Duff (1984), the alpha channel, i.e., the opacity of the combination of three images, can be computed by

$$\alpha = \mathrm{r} + \mathrm{g} + \mathrm{b} - \mathrm{rg} - \mathrm{rb} - \mathrm{gb} + \mathrm{rgb}$$

We are now searching for the R, G, and B values of the image [R, G, B, α] so that alpha blending above a black background falls back to the color composite [r, g, b]:

$$[\mathrm{r}, \mathrm{g}, \mathrm{b}] = \alpha[\mathrm{R}, \mathrm{G}, \mathrm{B}]$$

From this, it follows that the searched RGBα overlay image becomes

$[x \in [\mathrm{r}, \mathrm{g}, \mathrm{b}],\ g/\alpha,\ \mathrm{x} = \frac{x' - \min(x')}{\max(x') - \min(x')}]$, with α as defined above. Note that in digital image editing and computer graphics, the same result can be achieved with the "screen blending" technique.

In the special case of only 2 SALs, the possible color space consists of the fully opaque primary colors and their additive mixing colors.

To be able to distinguish between the combination color white (resulting of an additive mixing of the three principal colors red, green and blue) and the background of the figure, a checkered background has been added to the figures. We used a checkered background in order to demonstrate the method's ability to blend data fields on arbitrary backgrounds, e.g., according to their level of significance or importance. In principle, other backgrounds are also possible such as plane neutral colors (except for white), or an elevation map, etc.

For regions which are colored in one of the primary colors, the respective parameter is the only one fulfilling the pre-defined relevance criterion. For regions which are completely white, the pre-defined criterion is fulfilled for all three parameters. It is important to note that this is a fundamental difference compared to many other visualizations which usually use white as the color corresponding to the lowest or no value. For regions of purple color, only the "red" and the "blue" parameter fulfill the pre-defined criterion whereas for regions with yellow colors, only the red and the "green" parameters fulfill the pre-defined criterion. In turquoise regions, only the blue and green parameters fulfill the pre-defined criterion.

The colors assigned to the categories are not selected arbitrarily or by hand, but the combination and mixing of the colors is based on well-established methods and conventions from digital image editing and computer graphics. The advantage of this is that on the one hand, less "hand-work" is needed for the mapping of the categories to the specific colors and on the other hand, the primary colors and their mixing colors are widely used and especially the mixing colors can quickly be recognized and attributed to their respective primary colors. Also, the colors are well suited for being used on screens. One disadvantage might be that the selection of colors is fixed, and no adaptation of the colors with regard to content or visual disorders such as allochromasia is foreseen. However, for special applications, the method can be expanded to allow for the individual definition of specific colors mapped to the categories to be displayed.

Displaying changes of multiple climate parameters simultaneously and providing the option to integrate socio-economic data as well can illustrate possible interacting/interconnected conditions on one map, supporting the assessment of a variety of combined climate change impacts. In the following section, two examples of such combined-parameter maps will be given.

Application

Summer heat and intense precipitation days in populated areas

Already under today's climate conditions, urban population occasionally experiences extreme summer conditions, either due to extremely hot temperatures or through extreme precipitation events. The former are especially harmful to health when nighttime regeneration is prevented due to a lack of cooling during the night. The latter frequently causes damages in households and businesses and can lead to interruptions in public services such as transportation.

To assess the exposure of urban population to these two extreme summer conditions, today's population density (R) has been combined with the projected increase in the number of summer days during June, July, and August (JJA) showing precipitation amounts of more than 20 mm/day (G) and with the projected increase in the number of tropical nights, defined by a minimum daily temperature of at least 20 °C (B) (Figs. 2, 3, and 4). The pre-defined criterion chosen for the population density was set to values higher than 100 inhabitants/km^2 (subsequently referenced as high population regions). For tropical nights, an exceedance of twice the standard deviation of the occurrence of tropical nights in today's climate based on annual values is requested, and for intense summer precipitation days, the threshold is defined as an increase by more than 10%. For this example, two SALs are defined for the climatic parameters: opacity = 0: less than 66% of the simulations project changes fulfilling the pre-defined criterion (SAL "low"); opacity = 1: more than 66% of the simulations project changes fulfilling the pre-defined criterion (SAL "high").

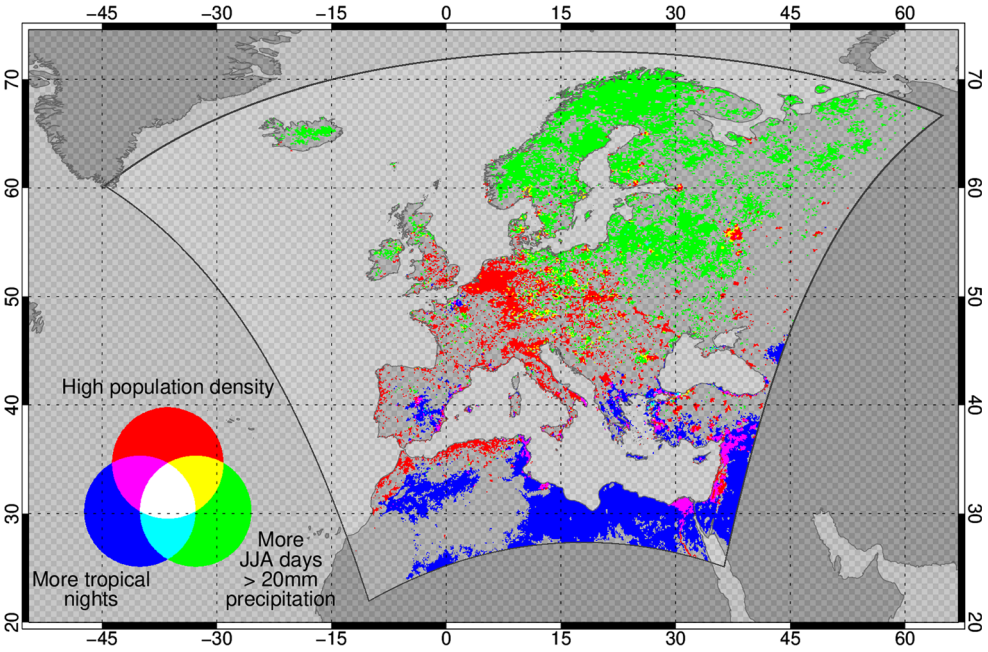

Fig. 2 Composite figure of population density > 100 inhabitants/km^2 (red), projected increase in tropical nights (blue) and projected increase in the number of summer days with precipitation of more than 20 mm/day (green) under 1.5 °C global warming conditions

As all three quantities can thus have values of only 0 ("No") and 1 ("Yes"), in total, 8 color states are available to describe all possible combinations (see Table 1).

Figures 2, 3, and 4 present the findings for the 1.5 °C, the 2 °C, and the 3 °C global mean temperature rise periods as defined in "Definition of the 1.5°C, 2°C, and 3°C global warming periods" section 2.3.

Looking at all three figures, it becomes clear that the increasing number of tropical nights (B) mainly affects Southern Europe and Northern Africa for the 1.5 °C warming period and stretches continuously northward when looking at the 2 °C (Fig. 3) and 3 °C (Fig. 4) warming periods. Opposite to this behavior, the trend of increasing numbers of intense precipitation days in summer (G) affects identical regions for all three global warming periods (Scandinavia, Eastern Europe, Scotland, Ireland, Iceland) but gets more comprehensive with higher global warming levels.

Consequently, there are no turquoise regions in Fig. 2), i.e., for the 1.5 °C global warming period, no regions are affected by increasing numbers of tropical nights and increasing numbers of intense precipitation days at the same time. For the 2 °C warming period (Fig. 3), some turquoise regions appear

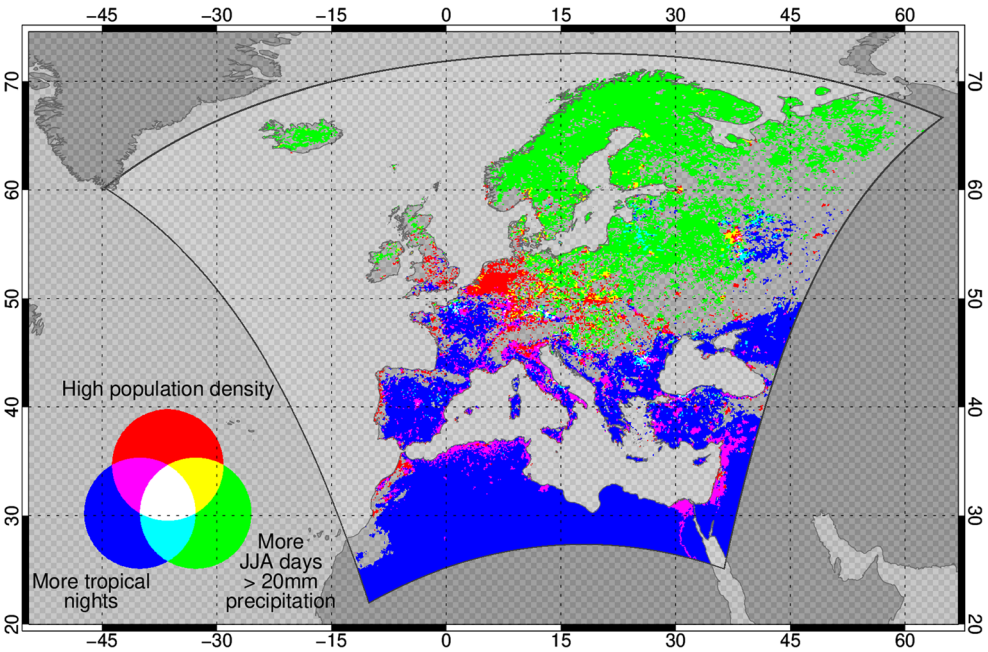

Fig. 3 Composite figure of population density > 100 inhabitants/km^2 (red), projected increase in tropical nights (blue), and projected increase in the number of summer days with precipitation of more than 20 mm/day (green) under 2.0 °C global warming conditions

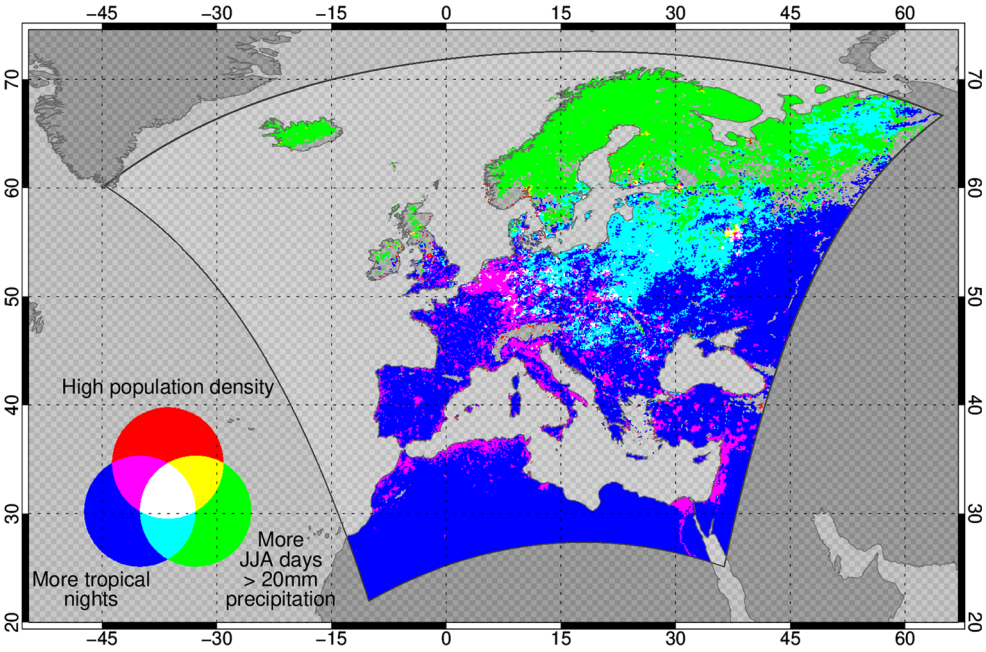

Fig. 4 Composite figure of population density > 100 inhabitants/km^2 (red), projected increase in tropical nights (blue) and projected increase in the number of summer days with precipitation of more than 20 mm/day (green) under 3.0 °C global warming conditions

in central and eastern Europe, which finally—under 3 °C global warming (Fig. 4)—stretch from eastern Germany across the Baltic States to north-western Russia.

When focusing on the population possibly affected by more extreme summer climate conditions, the magenta-, yellow-, and white-colored regions are essential.

Under 1.5 °C global warming conditions, highly populated areas are mainly affected by an increasing number of tropical nights in regions along the eastern Mediterranean coast and along the eastern coast of the Iberian Peninsula. The only high population region upcountry experiencing significant increases in the number of tropical nights already under 1.5 °C global warming conditions is the municipality of Madrid.

Under 2 °C global warming, the highly populated regions exposed to heat stress are clearly enlarged, covering most areas along the Mediterranean coast. Also, more inland regions appear in magenta, e.g., the Paris region, basically all large settlement areas in western Turkey, but also parts of south-western Germany. Also, under 2 °C global warming, some yellow regions emerge, where a high population density will be exposed to increasing numbers of intense summer precipitation days. These are mostly located in Central, Northern, and Eastern Europe.

Under 3 °C global warming, regions where many people are faced with significantly increasing numbers of tropical nights cover large parts of central Europe, most prominently along the line of the Benelux countries via the Alpine Ridge down to the Po valley. For 3 °C global warming, finally white regions emerge, located in Central Europe and also in the Moscow area at the borderline between regions with heat stress and regions with increasing intense precipitation. These highly populated regions would have to prepare for both heat-related and intense precipitation-related challenges if 3 °C global warming was reached.

Table 1 Detailed description of the color legend for example 1 (Figs. 2, 3, and 4)

Population density > 100inhabitants/km^2	Significant increases of tropical nights	> 10% more summer days with precipitation > 20 mm	Additive mixing color
No	No	No	Black (not shown / transparent)
Yes	No	No	Red
No	Yes	No	Blue
No	No	Yes	Green
Yes	Yes	No	Magenta
No	Yes	Yes	Turquoise
Yes	No	Yes	Yellow
Yes	Yes	Yes	White

In-depth assessment of the increase in summer temperature

The first example presented projected changes of two climate indices in combination with socio-economic data, which can provide information for practical applications such as the assessment of the number of people at risk for certain climatic impacts. However, the visualization method can also be useful for more research-driven purposes, e.g., for the assessment of the projected climatic changes of a specific feature (such as temperature) in more detail. This is illustrated with the second example: For summer temperatures, the mean daily temperature (tasmean) increase (R) has been combined with the daily maximum temperature (tasmax) increase (G) and the daily minimum temperature (tasmin) increase (B). The pre-defined criterion to be fulfilled was the exceedance of the standard deviation of today's climate by a factor of 2 (> 2sigma), to display statistically significant projected changes only. To account for the bandwidth of the ensemble of the projected climatic changes, four SALs were defined: opacity = 0: less than 50% of the simulations project changes fulfilling the pre-defined criterion (SAL no); opacity = 0.33: between 50% and 70% of the simulations project changes fulfilling the pre-defined criterion (SAL "low"); opacity = 0.66: between 70% and 90% of the simulations project changes fulfilling the pre-defined criterion (SAL "middle"); opacity = 1; more than 90% of the simulations of the ensemble project changes fulfilling the pre-defined criterion(SAL "high"). Note that with this additional level of information, the theoretical color range is extended to 27 possible colors including 2 levels of gray for identical SALs for all parameter projections. White color indicates a high SAL for all three parameters at once.

For the 1.5 °C period (Fig. 5), the projected changes do not exceed double the standard deviation of present climate temperatures for large parts of central Europe. The blue colors in parts of Spain, Greece, southern Italy, Turkey, and Scandinavia indicate that the projected changes of the daily minimum temperature here exceed the > 2sigma criterion. The magenta coloring in some parts of northern Scandinavia, Turkey, and northern Africa indicates that here, changes of tasmin as well as tasmean exceed the > 2sigma criterion.

For the 2 °C period (Fig. 6), the regions where the daily minimum temperature changes exceed the > 2sigma criterion are clearly enlarged, leaving only a small region in central Europe without significant changes of tasmin. Also, the magenta/purple regions now expand over the whole of Scandinavia in the north, the Alps, and along Spain, Greece, and Turkey in the south. The white color in northern Africa indicates that here, changes of all three temperature indices exceed the > 2sigma. This is again more pronounced in Fig. 7 for the 3 °C period, where this is the case for Turkey, Greece, southern Italy, Spain, and northern Scandinavia. Note that only low simulation agreement levels for significantly increasing tasmin, identifiable by the checkered background shining through, are reached for large parts of Scandinavia for 1.5 °C global warming (Fig. 5). These turn into a medium to high SAL for 2.0 °C global warming (Fig. 6) and finally into a high SAL for 3.0 °C global warming (Fig. 7), where the opacity of the blue component of all mixing colors appearing in Scandinavia equals 1. For 2 °C global warming, translucent regions of low SALs for significantly increasing tasmin still stretch from Ireland to Russia. For large parts of central Europe covering France, Germany, Poland, the Czech Republic, and Hungary, none of the three parameters change significantly with a SAL of more than 50%.

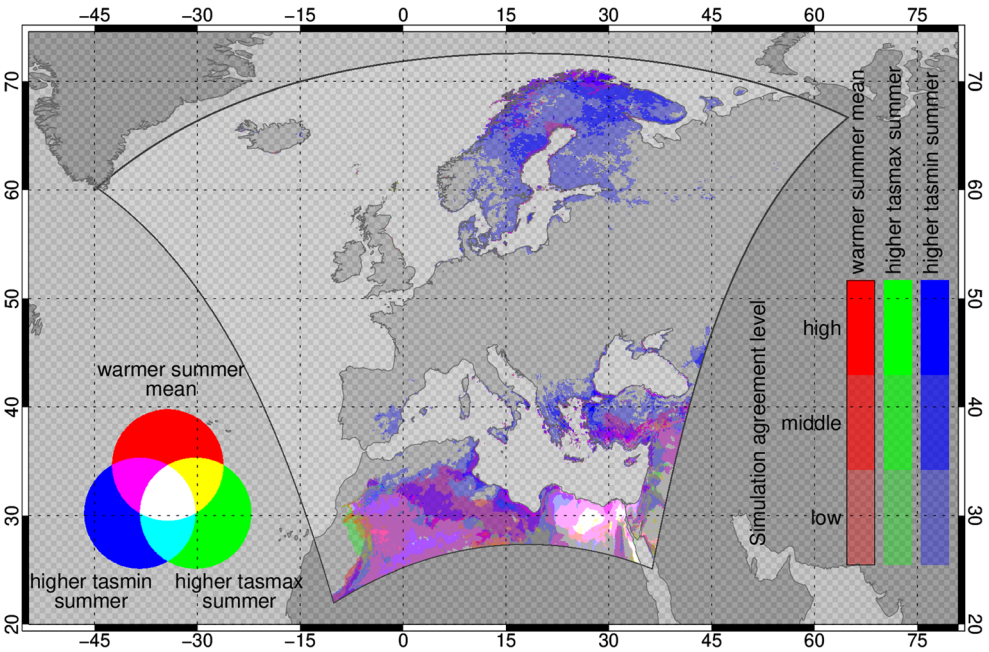

Fig. 5 Composite figure of projected increase in daily mean summer temperatures (red), projected increase in daily minimum temperatures (blue), and projected increase in daily maximum temperatures (green) under 1.5 °C global warming conditions

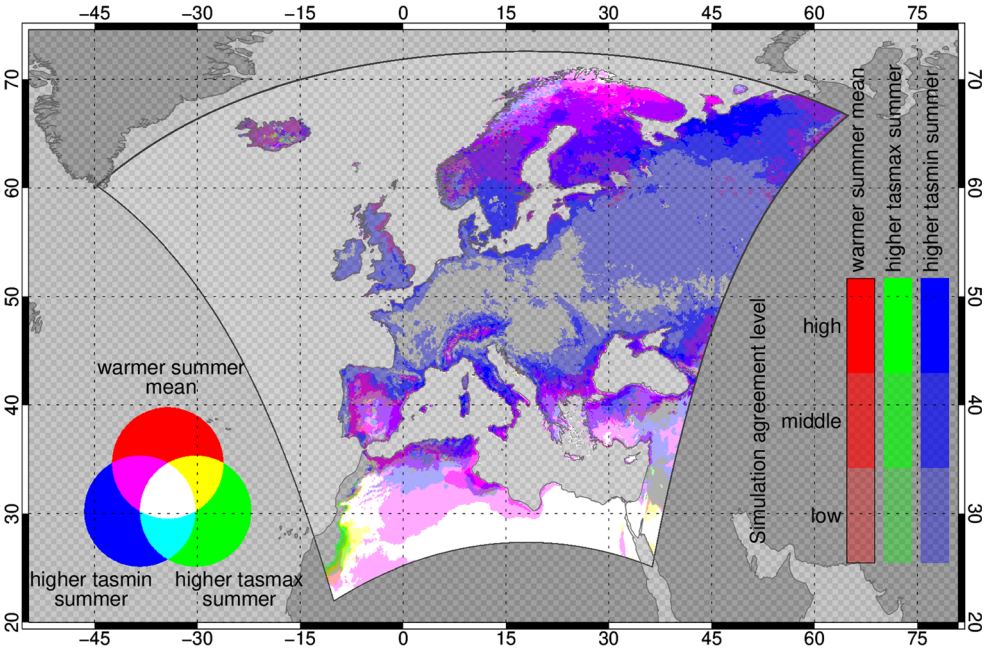

Fig. 6 Composite figure of projected increase in mean summer temperatures (red), projected increase in daily minimum temperatures (blue), and projected increase in daily maximum temperatures (green) under 2.0 °C global warming conditions

Under 3° global warming, there are only small regions in central Europe where the projected > 2sigma changes of tasmin do not suffice to raise the mean daily temperatures above the > 2sigma level (blue regions). The SALs are generally high, with the only small exception of central western Russia, where the checkered background shines through the magenta color indicating a low SAL of significantly increasing tasmean (R) together with a medium SAL of significantly increasing tasmin (B).

Summarizing, the maps for temperature show that the temperature increase for large parts of Europe is driven to a large extent by the increasing daily minimum temperatures. A pattern of change can be observed that intensifies from 1.5° to 3° warming: The strongest warming occurs in the northern and the southern parts of Europe, where with 3° global warming, a > 2sigma change of tasmin, tasmax, and tasmean can be seen. In contrast, central Europe is mostly affected by increasing daily minimum temperatures that drive the projected change in daily mean temperature. Here, even under 3° global warming, projected changes in daily maximum temperatures do not exceed the > 2sigma level. On the one hand, the different SALs can be used to highlight regions of very robust

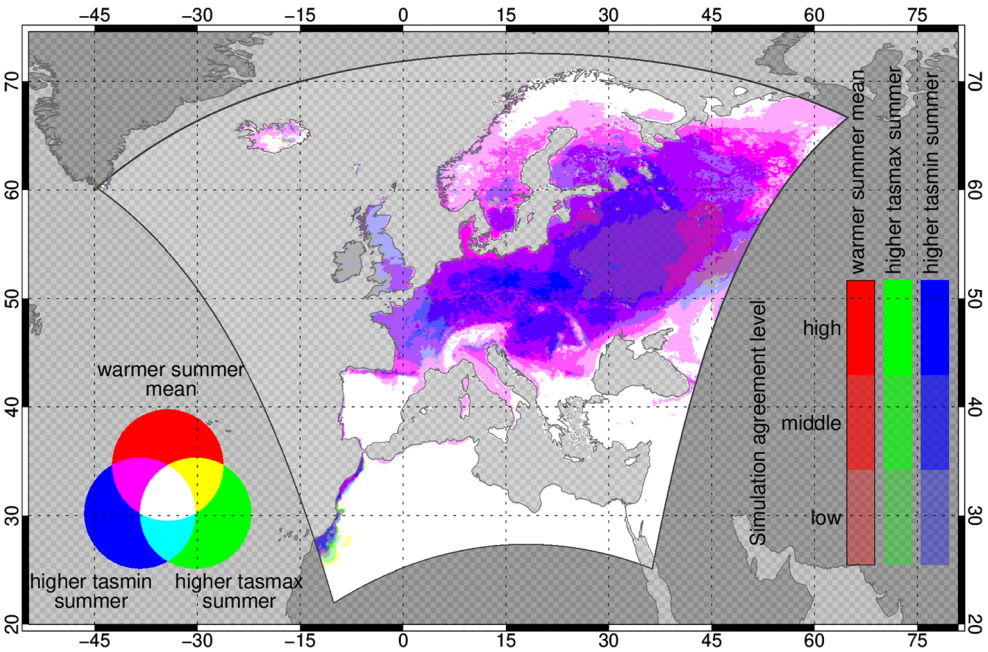

Fig. 7 Composite figure of projected increase in mean summer temperatures (red), projected increase in daily minimum temperatures (blue), and projected increase in daily maximum temperatures (green) under 3.0 °C global warming conditions

projections with SALs of 90% and more without omitting regions with medium to low SAL. On the other hand, looking at the three global warming levels, the different levels of SAL can give hints on whether observed features are getting more robust with rising global warming.

Discussion and conclusion

A method has been presented to detect multiple regional impacts of global climate changes. It allows studying projected future changes of three climatic parameters at once, as well as the combination of future changes of climatic parameters with socio-economic information. Additionally, the significance of the projected changes and the bandwidth of the ensemble projections can be considered.

With this, the visualization method shown here complements other visualization methods widely used, e.g., in the latest IPCC report (IPCC 2013), by providing quantitative, co-located information on multiple parameters and optionally their changes (concentrating on significant/relevant changes and including information on robustness of the projections) on a grid-box basis. To illustrate this, we compare our approach to two figures taken from the latest IPCC 5th assessment reports (AR5). In the first example shown in Fig. S1, the regions highlighted by hatching in both directions correspond to regions which would have a high SAL and would exceed the relevance criterion for one of the parameters shown in our figures. Similar figures were also shown recently by Kjellström et al. (Kjellström et al. 2018). Here, the main difference to our method is that our visualization offers the opportunity to assess different parameters at once, but restricts the presentation to significant/relevant changes only, while the IPCC figure concentrates on one parameter only, but displays the whole range of values, highlighting those areas where the projected changes (here of seasonal heavy precipitation) are significant/relevant and robust.

Another assessment of multiple parameters at once for specific regions is shown in Fig. S2, where qualitative information averaged over larger regions are given, but without information on the robustness and significance of the stated projected changes and without the possibility to assess regional to local co-occurrences of hot spots of the different parameters.

Our method thus offers a new way to clearly identify the areas affected by multiple changes, on only one map. No visual comparison using several maps is necessary. This, for instance, offers the possibility to compare extensions of areas affected by multiple changes for different warmer worlds. Clearly, set thresholds help interpret the changes that are shown and can be adjusted to individual needs. One clear disadvantage is, of course, the limitation of the method to three parameters only.

Two applications of the newly developed visualization method have been presented. The first showed a combination of high population density, increasing numbers of tropical nights and increasing numbers of intense summer precipitation days, highlighting that under 3 °C global warming, many heavily populated areas across Europe are affected by both heat stress and summer precipitation extremes, whereas under 1.5 °C global warming, heat stress regions are restricted to southern Europe and the large settlements along the Eastern Mediterranean coast. For the second example, the projected changes of mean, minimum, and maximum daily temperatures were shown in combination. Here, the visualization of low, medium, and high simulation agreement levels for significant projected future changes reveals increasing robustness of the projected temperature signals for the 3 °C global warming period as compared to the 1.5 °C and 2 °C periods. Also, by combining the three temperature parameters, it could be shown that the warming of the mean daily summer temperature is mainly driven by increasing daily minimum (i.e., night) temperatures.

Further to the application shown here, the method can be expanded and fine-tuned. Instead of presenting three independent variables, the findings of a study analyzing the development of the causal relationship between three connected parameters can be displayed this way. Concentrating on the three different global warming levels of 1.5 °C, 2 °C, and 3 °C, the method could also support the analysis of one parameter across these three scenarios, possibly revealing a non-linear relationship to the temperature variable or highlighting potential climate change impacts that can be avoided when limiting the global warming to 1.5 °C or 2 °C. Instead of focusing on the idealized scenarios showing the different global warming levels of 1.5 °C, 2 °C, and 3 °C, one could additionally compare different time periods, e.g., current climate and near and far future projections.

The combination of climatic and non-climatic elements has been presented with the first example where today's population density was integrated as one parameter to display the number of people at risk for a certain climatic impact. In the same way, possible future changes of other socio-economic values and also environmental changes can be incorporated. This way, the development over time for both the climatic change and non-climatic changes can be made visible, focusing on their superposition in a unique visualization method. Other statistical, demographical, or bio geographical values can be added, too, turning this method into a powerful tool for impact modelers.

Our method enables us to visualize regional detail from high resolution climate information, and to combine it with detailed spatial information of socio-economic data, or detailed human land use data, ecological data etc. Having comparable resolution available for all three parameters shown in the figures allows for meaningful regional to local assessments. For this reason, we used the spatially high resolved regional climate projection ensemble from EURO-CORDEX. With increasing availability of spatially high resolved climate projections from Global Climate

Models, this approach becomes also interesting and applicable on a global scale.

Assessing the changes of multiple climate-relevant variables affecting one region over the same time period is a crucial aspect to support climate adaptation action. Many different facets need to be considered simultaneously when developing a strategy and specific measures to cope with climate change. This method offers a multi-functional technique to investigate three elements in combination, advancing the preparedness for the changes to be expected in the future.

Acknowledgements We acknowledge the World Climate Research Programme's Working Group on Regional Climate and the Working Group on Coupled Modeling, the former coordinating body of CORDEX and the panel responsible for CMIP5. We also thank the climate modeling groups for producing and making available their model output. We also acknowledge the Earth System Grid Federation infrastructure, an international effort led by the US Department of Energy's Program for Climate Model Diagnosis and Intercomparison, the European Network for Earth System Modeling, and other partners in the Global Organization for Earth System Science Portals (GO-ESSP).

The authors acknowledge the contributing climate modeling centers for the EURO-CORDEX simulations and for making them freely available.

The population density data was provided by the Center for International Earth Science Information Network—CIESIN—Columbia University.

We gratefully acknowledge the helpful comments from the two anonymous reviewers that improved the paper significantly.

References

CIESIN (2016) "Gridded Population of the World Version 4 (GPWv4): Population Density, Beta Release." Center for International Earth Science Information Network. Palisades, NY: NASA Socioeconomic Data and Applications Center (SEDAC). https://doi.org/10.7927/H4D50JX4

Doxsey-Whitfield E, MacManus K, Adamo SB, Pistolesi L, Squires J, Borkovska O, Baptista SR (2015) Taking advantage of the improved availability of census data: a first look at the gridded population of the world, version 4. Pap Appl Geogr 1 (3). Routledge: 226–34. https://doi.org/10.1080/23754931.2015.1014272

IPCC (2013) Climate Change 2013: The Physical Science Basis. In: Stocker TF, Qin D, Plattner G-K, Tignor M, Allen SK, Boschung J, Nauels A, Xia Y, Bex V, Midgley PM (eds) Contribution of Working Group I to the Fifth Assessment Report of the Intergovernmental Panel on Climate Change. Cambridge University Press, Cambridge, 1535 pp. https://doi.org/10.1017/CBO9781107415324

IPCC (2014) Climate change 2014: impacts, adaptation, and vulnerability. In: Barros VR, Field CB, Dokken DJ, Mastrandrea MD, Mach KJ, Bilir TE, Chatterjee M, Ebi KL, Estrada YO, Genova RC, Girma B, Kissel ES, Levy AN, MacCracken S, Mastrandrea PR, White LL (eds) Part B: regional aspects. Contribution of Working Group II to the Fifth Assessment Report of the Intergovernmental Panel on Climate Change. Cambridge University Press, Cambridge, p 688. https://doi.org/10.1017/CBO9781107415386

Jacob D, Petersen J, Eggert B, Alias A, Christensen OB, Bouwer LM, Braun A, Colette A, Déqué M, Georgievski G, Georgopoulou E, Gobiet A, Menut L, Nikulin G, Haensler A, Hempelmann N, Jones C, Keuler K, Kovats S, Kröner N, Kotlarski S, Kriegsmann A, Martin E, van Meijgaard E, Moseley C, Pfeifer S, Preuschmann S, Radermacher C, Radtke K, Rechid D, Rounsevell M, Samuelsson P, Somot S, Soussana J-F, Teichmann C, Valentini R, Vautard R, Weber B (2014) EURO-CORDEX: new high-resolution climate change projections for European impact research. Reg Environ Chang 14(2):563–578. https://doi.org/10.1007/s10113-013-0499-2

Kjellström E, Nikulin G, Strandberg G, Christensen OB, Jacob D, Keuler K, Lenderink G, van Meijgaard E, Schär C, Somot S, Sørland SL, Teichmann C, Vautard R (2018) European climate change at global mean temperature increases of 1.5 and 2 °C above pre-industrial conditions as simulated by the EURO-CORDEX regional climate models. Earth Syst Dynam 9:459–478. https://doi.org/10.5194/esd-9-459-2018

Kotlarski S, Keuler K, Christensen OB, Colette A, Déqué M, Gobiet A, Goergen K, Jacob D, Lüthi D, van Meijgaard E, Nikulin G, Schär C, Teichmann C, Vautard R, Warrach-Sagi K, Wulfmeyer V (2014) Regional climate modeling on European scales: a joint standard evaluation of the EURO-CORDEX RCM ensemble. Geosci Model Dev 7:1297–1333. https://doi.org/10.5194/gmd-7-1297-2014

Leonard M, Westra S, Phatak A, Lambert M, van den Hurk B, Mcinnes K, Risbey J, Schuster S, Jakob D, Stafford-Smith M (2014) A compound event framework for understanding extreme impacts. Wiley Interdiscip Rev Clim Chang 5(1):113–128. https://doi.org/10.1002/wcc.252

Olesen JE, Trnka M, Kersebaum KC, Skjelvåg AO, Seguin B, Peltonen-Sainio P, Rossi F, Kozyra J, Micale F (2011) Impacts and adaptation of European crop production systems to climate change. Eur J Agron 34(2):96–112. https://doi.org/10.1016/j.eja.2010.11.003

Porter T, Duff T (1984) Compositing digital images, Proceedings of the 11th annual conference on Computer graphics and interactive techniques 253–259. https://doi.org/10.1145/800031.808606

Poumadère M, Mays C, Le Mer S, Blong R (2005) The 2003 heat wave in France: dangerous climate change here and now. Risk Anal 25(6): 1483–1494. https://doi.org/10.1111/j.1539-6924.2005.00694.x

Ritzema HP, Van Loon-Steensma JM (2017) Coping with climate change in a densely populated Delta: a paradigm shift in flood and water management in the Netherlands. Irrig Drain 67:52–65. https://doi.org/10.1002/ird.2128

Schleussner C-F, Rogelj J, Schaeffer M, Lissner T, Licker R, Fischer EM, Knutti R, Levermann A, Frieler K, Hare W (2016) Science and policy characteristics of the Paris agreement temperature goal. Nat Clim Chang 6(9):827–835. Nature Publishing Group, a division of Macmillan Publishers Limited. All Rights Reserved. https://doi.org/10.1038/nclimate3096

van Vuuren DP, Edmonds J, Kainuma M, Riahi K, Thomson A, Hibbard K, Hurtt GC, Kram T, Krey V, Lamarque J-F, Masui T, Meinshausen M, Nakicenovic N, Smith SJ, Rose SK (2011) The representative concentration pathways: an overview. Clim Chang 109(1):5–31. https://doi.org/10.1007/s10584-011-0148-z

Vautard R, Gobiet A, Sobolowski S, Kjellström E, Stegehuis A, Watkiss P, Mendlik T, Landgren O, Nikulin G, Teichmann C, Jacob D (2014) The European climate under a 2 °C global warming. Environ Res Lett 9(3):34006. https://doi.org/10.1088/1748-9326/9/3/034006

Zscheischler J, Seneviratne SI (2017) Dependence of drivers affects risks associated with compound events. Sci Adv 3(6):e1700263. https://doi.org/10.1126/sciadv.1700263